The Dust Environment of Comets 22P/Kopff and 81P/Wild 2

F. Pozuelos (1), F. Moreno(1) , F. Aceituno (1), V. Casanova (1), A. Sota (1) J. Castellano(2) and E. Reina (2)

(1) Instituto de Astrofísica de Andalucía, CSIC, PO Box 3004, 18008 Granada, Spain.

(2) Amateur Association Cometas-Obs

Abstract

In this work we present optical observations and Monte Carlo models of the dust environment of comet 22P/Kopff and a preliminary study of 81P/Wild 2. For the first one, we derived the dust loss rates, ejection velocities, and power law size distribution as functions of the heliocentric distance using pre- and post-perihelion imaging observations during the 2002 and 2009 apparitions. The best fit obtained is for an anisotropic ejection model. The asymmetries are inbound at $r_h = 2.5AU$ and outbound at $r_h = 2.6AU$ and they are compatible with a scenario where dust ejection is mostly seasonally-driven, coming mainly from regions near subsolar latitudes at far heliocentric distances inbound and outbound but at intermediate to near-perihelion distances, the outgassing would affect much more extended latitude regions becoming nearly isotropic. The model has also been extended to the thermal infrared to be applied to available trail observations with IRAS and ISO spacecrafts of this comet. The resulting trail intensities are in good agreement with those observations, which is remarkable taking into account that those data are sensitive to dust ejection patterns corresponding to several orbits before the 2002 and 2009 apparitions. For 81P/Wild 2 we run more than 8000 parameters combination for an isotropic particle emission pattern in a first step but an anisotropic ejection model is required to fit the complex structure shown by the comet. We include a rotating nucleus with active areas on it. In addition, we also include the asymmetry in the dust parameters respect to perihelion.

Results & Conclusions

We assume that the dust particles are described by spherical particles of density of $\rho = 1000\ kg\ m^{-3}$ and glassy carbon composition (refractive index at red wavelengths of $m = 1.88 + 0.71i$).

A. 22P/Kopff

*The nucleus size is $R_n = 1.8\ km$ and the geometric albedo is assumed $p_v = 0.036$ [2].

* Asymmetric and anisotropic ejection model.

*Rotating spherical nucleus with active areas on it, with a rotation period of 12.3 hours [3]. The best rotational parameters found, previously described by [6] are $\Phi = 180°$ and $I = 60°$.

*The location of the active area is found to correlate with the subsolar point position (Figure 1). The fraction of particles ejected isotropically, and the cone width were derived as $\Delta\phi = 60°$ for $r_h > 2.5AU$ pre-perihelion with no need for an isotropic ejection fraction and $\Delta\phi = 20°$ for $r_h > 1.95AU$ post-perihelion and 30% of particles being emitted isotropically.

* The modeled intensities are in agreement with ISOCAM observations at $\delta MA = +0.5°$, and at $\delta MA = +1.0°$, while the trail widths are significantly narrower than reported by [4]. However, they are similar to IRAS data [5] when re-analyzed by [4].

* The size distribution function is independent of the heliocentric distance, characterized by a constant power index of -3.1

* Minimum and maximum particle radius between $1\mu m$ and $1\ cm$.

*The results of the synthetic isophotes compared with observations are shown in the figure 3.

*The total mass ejected per orbit is $8x10^9\ kg$, with and average dust mass lost rate per orbital period of $40\ kg\ s^{-1}$ or $1.3x10^9\ kg\ yr^{-1}$. The maximum dust loss rate is about $260\ kg\ s^{-1}$ at perihelion.

B. 81P/Wild 2

*Only preliminary results are reported because the work is still going on.

*The nucleus size is near $R_n = 2.1\ km$ and the geometric albedo is $p_v = 0.040$ [6].

*With an isotropic and symmetrical particle emission model we estimate the lower and upper limits for the dust parameters. From our current simulations we obtain the dust loss rate in the range $1000 - 2000\ kg\ s^{-1}$, a maximum size of particles around $1 - 3\ cm$, and ejection velocities for particles of $1\ cm$ between $2 - 4\ m\ s^{-1}$ at perihelion.

* An anisotropic and asymmetrical ejection model will be implemented to improve the results. We include a rotating nucleus with actives areas on it with a rotation period of 13.7 hours [7]. The fit shown in figure 4 corresponds to rotational parameters $\Phi = 180°$ and $I = -30°$ with an active area located between $0° - 30°$ and the particles ejected isotropically 45%. The size distribution function is independent of the heliocentric distance, characterized by a constant power index of −3.

Observations

Most of the observations of both comets were taken by the 1.52-m telescope of Sierra Nevada Observatory (OSN) in Granada, Spain. We have also benefited from amateur observations carried out by the astronomical association *Cometas-Obs*, providing a CCD lightcurve and $Af\rho$ measurements as a function of the heliocentric distance. For 22P/Kopff we considered coma/trail images obtained at large heliocentric distance by Masateru Ishiguro at Kiso 1.05-m Schmidt telescope in Nagano, Japan, and Canada-France-Hawaii 3.6-m telescope (CFHT) [1].

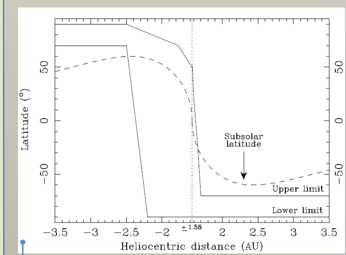

Fig. 1. 22P/Kopff. Upper and lower latitude boundaries of the active area as a function of the heliocentric distance. Also displayed is the latitude of the subsolar point, which shows a similar behavior with time.

Parameter	Value adopted/retrieved
Grain density	1000 kg m^{-3}
Grain refractive index	m=1.88+0.71*i*
Grain geometric albedo	p_v=0.036
Ejection velocity	$v(t,\beta) = v_1(t)\beta^{1/2}$, see Fig. 6
Peak ejection velocity of 1-cm grains	2.7 m s^{-1}
Size distribution: r_{min}, r_{max}	10^{-4} cm, 1.4 cm
Size distribution: Power index	-3.1
Peak dust mass loss rate (perihelion)	260 kg s^{-1}
Averaged dust mass loss rate per orbit	40 kg s^{-1}
Total dust mass ejected per orbit	8×10^9 kg
Pre-perihelion switch-on activity	$r_h \gtrsim 3.5$ AU
Nucleus rotation period	12.3 h (Lowry and Weissmann, 2003)
Argument of subsolar meridian at perihelion	Φ=180°
Obliquity	*I*=60°
Active area location	Time-dependent, see Fig. 12
Cone angle width	$\Delta\phi$=60° for r_h >2.5 AU pre-perihelion
	$\Delta\phi$=20° for r_h >1.95 AU post-perihelion
	$\Delta\phi$=40° otherwise
Isotropic emission percentage	30%

Tab. 1. Model physical parameters for 22P/Kopff

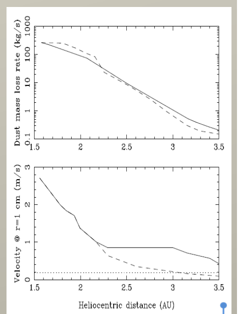

Fig. 2. 22P/Kopff. Upper panel: Dust mass loss rate of heliocentric distance. lower panel: ejection velocity of r=1 cm glassy carbon spheres as a function of heliocentric distance. In both panel, the solid line corresponds to pre-perihelion, and the dashed line to post-perihelion.

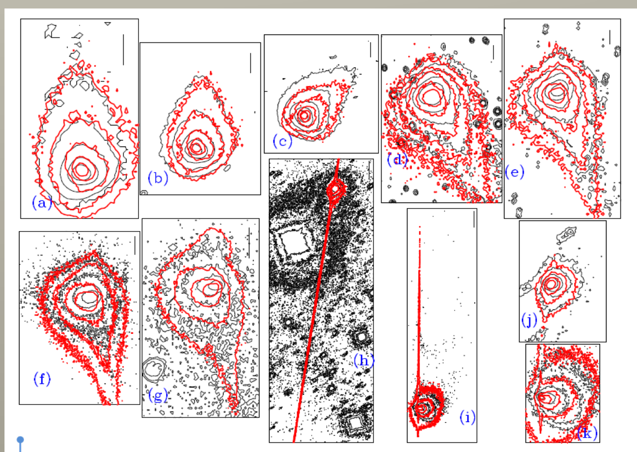

Fig. 3. 22P/Kopff. Results of anisotropic and asymmetric model. Thin (black) contours are the observations and thick (red) contours, the model. Images from (a) to (g) correspond to the 2009 apparition taken at Sierra Nevada Observatory. The observations date are: (a), 2009-07-31; (b), 2009-08-15; (c), 2009-08-28; (d), 2009-09-21; (e), 2009-10-12; (f), 2009-11-09; (g), 2009-11-24. Panel (h) corresponds to Kiso Observatory on 2002-05-12, and the panel (i) corresponds to the CFHT observation on 2003-07-31. Panels (j) and (K) are zoomed regions of images (h) and (i) near the coma regions.

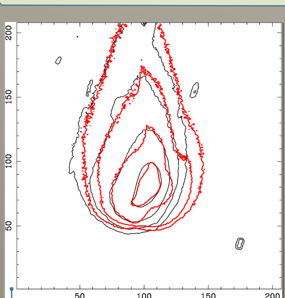

Fig. 4. 81P/Wild 2. Anisotropic and asymmetric model. Thin (black) contours are the observations and thick (red) contours, the model. The image corresponds to the 2010 apparition, and was taken at Sierra Nevada Observatory. The observation date is 2010-03-09.

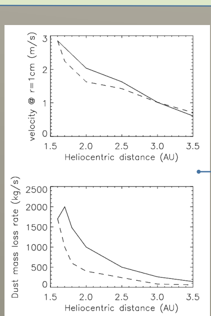

Fig. 5. 81P/Wild 2. Lower panel: Dust mass loss rate vs heliocentric distance. upper panel: ejection velocity of r=1 cm glassy carbon spheres as a function of heliocentric distance. In both panel, the solid line corresponds to pre-perihelion, and the dashed line to post-perihelion.

Obtain the full article version "Comet 22P/Kopff: Dust environment and grain ejection anisotropy from visible and infrared observations". (Moreno et al. 2012)

References

[1] Ishiguro, M., Sarugaku, Y., Ueno, M., Miura, N., Usui, F., Chun, M.-Y., and Kwon, S.M., 2007, Icarus, 189, 169

[2] Lamy, P.L., Toth, I., Jorda, L.,Groussin, O., A'Hearn, M.F, Weaver, H.A., 2002, Icarus, 156, 442

[3] Lowry, S.C., Weissman, P.R., 2003, Icarus, 164, 492

[4] Davis, J.K., Sykes, M.V., Reach, W.T., et al., 1997, Icarus, 127, 251

[5] Sykes, M.V., & Walker, R.G., 1992, Icarus, 95, 180

[6] Brownlee, D.E., et al., 2004, Science, 304, 1764

[7] Muller, B.E.A., et al., 2010, BAAS, 42, 966